# On-line PD measuring system for MV cables : some practical aspects and implications

XIIIth International Symposium on High Voltage Engineering, Netherlands 2003, Smit (ed.)


# On-line PD measuring system for MV cables: some practical aspects and implications

P.A.A.F. Wouters, P.C.J.M. van der Wielen, J. Veen and E.F. Steennis
Eindhoven University of Technology, Netherlands

**Abstract:** In this paper the implications of substations as the termination impedance of a medium voltage cable is studied. This impedance is not only a decisive factor in choosing optimal coupling schemes for PD sensors, but also determines which solutions are feasible for communication and synchronization between PD detection sites at both cable ends. The effective impedance resulting from a distribution transformer corresponds to typically a 1 nF capacitance for frequencies within the CENELEC A-band allowed for communication. Coupling efficiency is the main obstacle for reliable communication by means of inductive coupling, since attenuation during signal propagation is relatively low: about a factor two at 100 kHz for a 4 km paper-oil insulated three-phase belted cable. Interpretation of PD distributions depend on the eccentricity of the elliptical field within a three-phase belted cable, and thus on the location of the defect but also on the phase angle of the applied field. This results in a modification of the PD patterns as compared to off-line tests with only one phase energized.

## 1. Introduction

Partial Discharge (PD) localization techniques in medium voltage (MV) cables require two signals originating from a defect that travel in both directions. For an off-line test, one end is usually left open and it reflects the signal completely back to the other side where the time difference is obtained. During an on-line measurement, however, the impedances at the cable terminals depend on the electric properties of the substation with impedances of other cables, the transformer impedance, and maybe also a signal propagation delay inside the substation due to its finite size. In this case, the reflected signal is distorted and often hardly visible. Therefore, signal detection at both ends is preferred for on-line PD localization. As a consequence, information must be transferred between both sides and the equipment must be synchronized. In principle, communication can be realized via a telephone connection, and synchronization by GPS. These options are not always practical solutions, e.g. GPS requires a direct satellite connection, which can be hampered by surrounding buildings. The cable under test can serve as a channel to perform these tasks as well. The performance of this channel depends on the cable propagation properties and the properties of the substations "loading" the cable for the frequency range of interest. Clearly, this information is relevant as well for the more basic monitoring tasks, namely PD sensing and optimising signal processing. In section 2 the behaviour of this channel is studied for frequencies relevant to communication (in Europe restricted by CENELEC standards, EN50065). For synchronization, short pulses containing frequencies in the MHz range can be used. Implications of the load formed by a substation on these signals are briefly discussed in section 3.

On-line measurement of signals in a three-phase belted cable does not only have implications on PD distributions itself due to the elliptical nature of the applied field, as discussed in [1]. Also signal coupling to the various conductors becomes dependent on the momentary phase angle as is discussed in section 4. Furthermore, such a cable acts as a multi-conductor transmission line with several propagation modes [2]. The detected signal is determined by the complete process of signal coupling at the discharge site up to decoupling the PD signal at the cable end. These aspects may differ from off-line PD detection [3].

## 2. Communication over MV cable

In the simplest form a MV connection between two substations consists of a cable, which is loaded at both ends by an impedance, Figure 1. This impedance can consist of a leaving cable to a subsequent line or power station or can be a distribution transformer or a combination of both. Also switchgears may contribute to the impedance. The leaving cable can be described by its characteristic impedance for long cables; for relatively short cables, the cable capacitance or inductance, together with the load at the other side, has to be taken into account. To get insight in the transformer behaviour, a 400-kVA 10kV/380V cast resin transformer has been investigated using a vector impedance bridge (HP4274A).

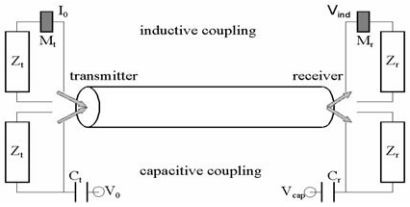


**Figure 1:** Capacitive coupling ($V_0$: injected voltage, $V_{cap}$: detected voltage) and inductive coupling ($I_0$: injected current, $V_{ind}$: detected induction voltage). Mutual inductances at transmitter and receiver side are denoted with $M_t$ and $M_r$ respectively; the capacitive coupling is realized through $C_t$ and $C_r$.

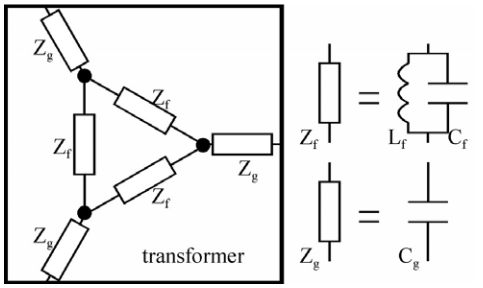


**Figure 2:** Representation of a three-phase transformer as lumped components for a 120° rotation symmetrical system.

For the frequency range of interest (up to 100 kHz) the transformer is modelled with lumped impedances $Z_f$ between the phases and impedances $Z_g$ from one phase to ground, as depicted in Figure 2. $Z_f$ consists of a coil inductance parallel to a capacitance, which takes into account the capacitive coupling of the windings; $Z_g$ corresponds to the capacitance between coil and transformer core/housing. The results for two tested configurations are shown in Figure 3: (a) impedance between three connected phases and ground, and (b) impedance between one phase and ground with the other two phases floating. The curves in Figure 3 are fits using $C_g$=315 pF, $C_f$=260 pF, and $L_f$=17 H or 0.086 H depending on the load at the low voltage side (open or short circuit). For frequencies above about 50 kHz (right of the LC resonances in Figure 3b) the transformer behaves like a capacitor under all conditions.

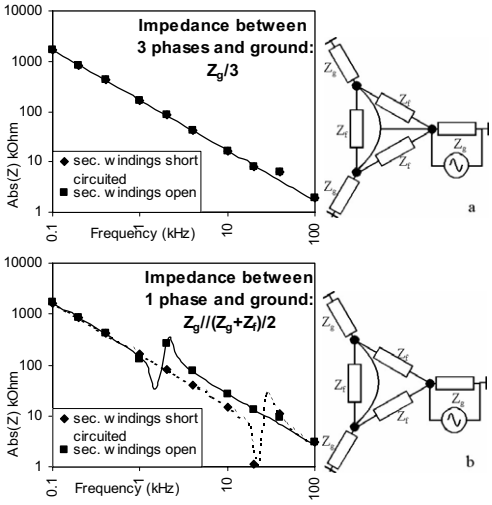


**Figure 3:** Transformer impedance between 100 Hz and 100 kHz for two situations: three phases connected with respect to ground (a) and one phase with respect to ground with two phases floating (b).

The effective impedance in a practical coupling scheme consists of a number of parallel channels; e.g. for inductive coupling in one phase the return path consists of the screen and both other phases. It is therefore expected that a distribution transformer typically behaves as a capacitor of the order of 1 nF. For transformers within a metal enclosure and for larger transformers, e.g. connecting the grid to transmission lines, this capacitance can be considerably higher.

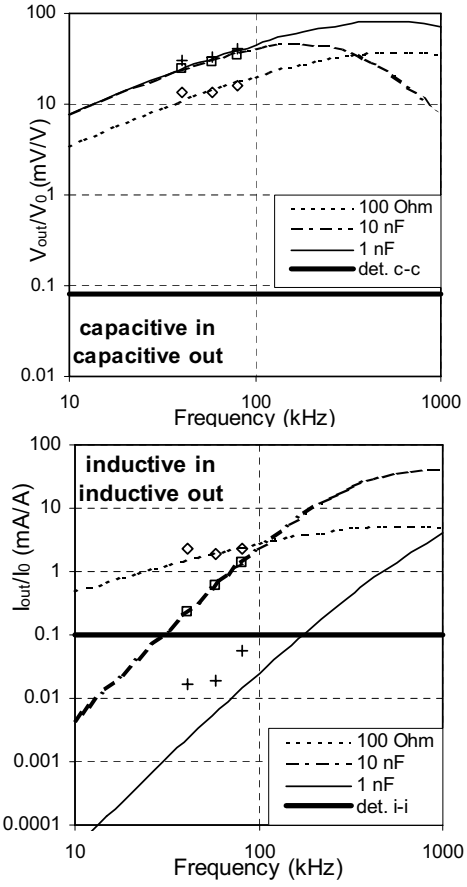


**Figure 4:** Extrapolation of the signal transfer according to (1) up to 1 MHz for capacitive and inductive coupling using various load conditions at both cable ends. The symbols are obtained from measured data.

A 4 km three-phase cable connection was used to measure the signal transmission properties. The cable was loaded on both sides with several impedances, resistive as well as capacitive, to mimic different load situations. Both inductive (air coil with mutual inductance of 1.86 μH) and capacitive (through a 2 nF capacitor) coupling have been investigated. In Figure 4 the results are shown, together with theoretical curves

based on two fit parameters obtained from the measurements, valid for all situations: cable impedance ($Z_0$=40 Ω), and damping factor ($\alpha(\omega)\ell=0.0010\sqrt{\omega}$). The transfer functions (ratio between current or voltage at the cable end and the injected current or voltage) are given by [4]:

$$\frac{I_{out}}{I_0} = \tfrac{1}{2}\frac{j\omega M_t Z_0}{Z_t(\omega)Z_r(\omega)} \cdot \tau_t(\omega)\cdot\tau_r(\omega)\cdot\frac{e^{-\gamma(\omega)\ell}}{1-\rho_t(\omega)\rho_r(\omega)e^{-2\gamma(\omega)\ell}} \quad (1)$$

$$\frac{V_{out}}{V_0} = \tfrac{1}{2} j\omega C_t Z_0 \cdot \tau_t(\omega)\cdot\tau_r(\omega)\cdot\frac{e^{-\gamma(\omega)\ell}}{1-\rho_t(\omega)\rho_r(\omega)e^{-2\gamma(\omega)\ell}}$$

The factors ρ and τ describe the frequency dependent reflection and transmission coefficients at the transmitting (index *t*) and receiving (index *r*) side. The propagation coefficient $\gamma(\omega)=\alpha(\omega)+j\beta(\omega)$ contains both attenuation $\alpha(\omega)$ and phase shift $\beta(\omega)$. Due to the signal attenuation forth and back the cable (8 km), the denominator of the last factor in (1) is approximately 1. The actual detected voltage, either capacitively $V_{cap}$ or inductively $V_{ind}$ (Figure 1), depends on details of the detection circuit, which are not included in (1). Load impedances of 100 Ω, 1 nF and 10 nF were chosen, as being indicative for the performance of the communication channel. The deviation between experimental results and the calculated curve for a 1 nF load can be explained by an extra capacitance present due to measuring cables. It must be noted that the curves are extrapolated to 1 MHz. A transformer will not behave as a perfect capacitor over this frequency range, but may exhibit some internal LC resonances. By means of FSK (Frequency Shift Keying) modulation the actual signal transmission was checked. The horizontal lines indicate the estimated sensitivity of the equipment used (which still can be improved).

From the results it is concluded that capacitive signal coupling should be preferred if only the technical performance is considered. However, inductive coupling remains interesting, because no galvanic contact with the energized phase conductors is required. At a load impedance from only a distribution transformer (typically 1 nF) the transmission is not guaranteed. For reliable inductive data transfer the coupling strength must be increased, either by injection coils with ferromagnetic cores or by frequencies extending up to 1 MHz. At present the CENELEC allows only frequencies up to 95 kHz for utilities, but possibly this changes in the near future.

## 3. Synchronization by pulse injection

A time resolution for synchronization of about 100 ns is required for localization of a PD spot within about 10 m. To obtain this resolution, pulses serving as time label can be injected at one side. For the pulse duration a compromise has to be found: on one hand very short pulses result in perfect time definition, but on the other hand the high frequencies attenuate more during signal propagation. Another important aspect is the pulse injection method. Inductive coupling is preferred for practical reasons as was the case for communication. A well-defined pulse can be realized, e.g. by discharging a capacitor with suitable value over the self-induction of the injection coil. A (MOSFET) switch in the circuit blocks the resulting oscillation at a desired time, e.g. after a half cycle, Figure 5 (top). The impedances present in the substation, however, determine the current waveform in the secondary circuit, because the injection coil forms a weakly coupled transformer with the substation. The signal is distorted and the obtainable time resolution is reduced. The distortion also contains valuable information on the relevant impedances in the substation itself. On-line measurement of the response on injected pulses may actually help to interpret real PD signals, as the bandwidth of interest for both PD signals and synchronization pulses essentially coincides.

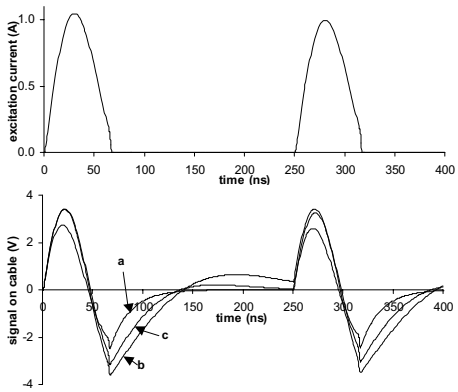


**Figure 5:** Top: simulated excitation waveform with 1 A amplitude. Bottom: voltage over cable in secondary circuit formed by the substation with a load consisting of (a) cable, (b) transformer, or (c) both. The parameters are specified in the text.

In Figure 5 (bottom) the simulated injected current is shown for a few situations, namely two cables connected by a rail (5a), one cable connected to a transformer (5b), and two connected cables with one transformer in between (5c). A value of 2 μH is estimated for the self-induction of the connection. The transformer is modelled as a capacitance of 1 nF, as discussed in the previous section. The coil used has a mutual inductance of 0.2 μH, and was energized by a 1 A injection current. The responses shown should only be considered as indicative, since practical substation impedances require more sophisticated modelling. Despite the distortion, the synchronization can still be established with sufficient accuracy.

## 4. Implications for multi-conductor MV cable

In The Netherlands three-phase belted cables are used extensively. During operation the electric field in the

cable, but especially in cable joints, is elliptical, which is shown in Figure 6 for an artificial cable (joint) geometry. Because of the large difference between the time scale of an actual PD (ns) and the time scale associated with the detection bandwidth (MHz), a PD can be considered as a sudden emergence of a dipole field somewhere in the dielectrics. For a small spherical void with radius $a$, assuming the PD will neutralize the electric field within the void, we can replace the charge redistribution by introducing a dipole $p$ [3]:

$$\vec{p} = Q_{real}\vec{d} \quad \text{with} \quad Q_{real} = 3\pi\varepsilon a^2 E_0 \quad \text{and} \quad d = \tfrac{4}{3}a \qquad (2)$$

with ε the permittivity of the dielectrics and $E_0$ the applied electric field in the void.

According to Ramo Shockley theory (see e.g. [5]) the induced charge $Q_{app}$ upon a PD with charge $Q_{real}$ at one conductor can be calculated just by considering the Ramo Shockley field strength $E_{RS}$ at the PD site, which would arise when that specific conductor is energized with voltage $U_A$, and all other conductors are grounded [3]:

$$\frac{Q_{app}}{Q_{real}} = -\frac{\vec{E}_{RS}\cdot\vec{d}}{U_A} \qquad (3)$$

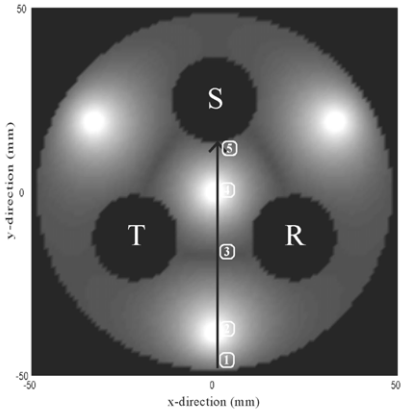


**Figure 6:** Eccentricity of the electric field in a hypothetical cable joint configuration. The light circular areas (e.g. at positions 2 and 4) indicate regions with circular field. Linear fields are found close to the conductors and on the dark areas between two conductors (along y-direction at positions 1 and 5; along x-direction at position 3). The path indicated by the black arrow and the numbering correspond to results shown in Figures 7 and 8.

In Figure 6 the path is shown along which the induced charge upon a PD is calculated for Figure 7. Some specific locations are indicated where the electric field either is linear (1 and 5: field along y-axis; 3: field along x-axis) or circular (2 and 4). In between the field is elliptical. Along the path the real charge and the induced charge in the cable earth screen are shown for PDs directed either in x- or y-direction. This is of particular interest because (inductive) PD signal extraction from the cable screen is from an operational point of view preferred above any detection method involving coupling to an energized phase conductor. Although the field along the x-axis may be larger in some areas, PDs occurring in that specific direction remain undetected, because no charge is induced in the screen. Specifically, position 3 (linear field in x-direction) will not result in detectable PDs at the earth screen. The induced charge in the cable centre is zero as well, due to the cable (or joint) geometry.

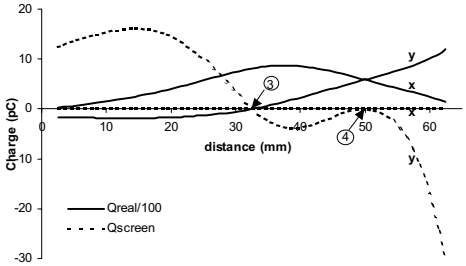


**Figure 7:** Real charge and induced charges in the earth screen from a PD along the x- and the y-direction calculated along the path shown in Figure 6 for a 50 mm$^3$ spherical void. Numbers 3,4 correspond to positions indicated in Figure 6.

In Figure 8 the calibration factor (defined here as ratio between apparent charge induced in the earth screen and real charge) is plotted for the positions in the dielectrics indicated in Figure 6 as a function of the phase angle. In case of a linear field (positions 1 and 5) this factor switches between plus and minus the extreme value. For elliptical fields this factor only gradually changes with phase angle (position 2). "Blind spots", i.e. regions from which no charge is induced in the earth screen, arise at a narrow region around position 3 (field aligned along x-direction) and near the cable centre at position 4 (due to the cable geometry).

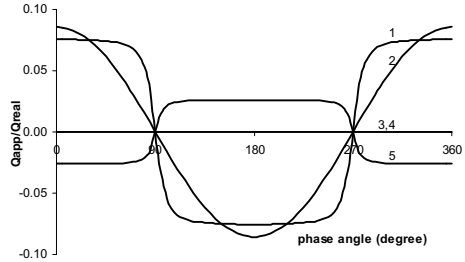


**Figure 8:** Calibration factor between apparent and real charge at the various locations indicated in Figure 6 as a function of phase angle (referred to phase S). Numbers 1-5 correspond to positions indicated in Figure 6.

## 5. Discussion and conclusion

Sensors for on-line PD localization system should preferably perform additional tasks, e.g. synchronization and communication. The detection bandwidth

both for optimal PD sensing and for injecting/detecting synchronization signals are comparable and can therefore be combined. As long as the CENELEC standard restricts the communication band to about 100 kHz, incorporation of this task in the same sensor, especially when inductive coupling is applied, is not straightforward. The communication frequency range is considerably lower, resulting in other design parameters for the injection coil.

Applying a synchronization pulse results in an injected waveform in the cable that depends on the configuration of the substation. This distorts the signal, but also contains valuable information on the state of the substation. Usually, a distribution grid is a ring with an opened switch somewhere, depending on its history. Intelligent PD monitoring requires that the actual configuration is known, e.g. by extracting this information from the synchronization pulses.

For PD detection in a three-phase belted cable, a suitable sensor location has to be chosen. If the signal is only measured at one conductor, e.g. the earth screen, information is lost if no charge is induced there. The structure of real defects in paper-insulated cables extends over a relatively large area. Because the "blind spots" mentioned in section 4 are very localized, real defects in that area may still be detected (with reduced amplitude) using the earth screen current as the only source for PD signal detection.

## 6. Acknowledgement

This research is supported by the following Dutch parties: Technology Foundation STW, applied science division of NWO and the technology programme of the Ministry of Economic Affairs; Eindhoven University of Technology; KEMA Nederland B.V.; N.V. Continuon Netbeheer; REMU Infra N.V.

## 7. References

[1] P.C.J.M. van der Wielen, P.A.A.F. Wouters and E.F. Steennis, "Signal interpretation of partial discharges in three-phase medium voltage cable systems measured on-line", IEEE International Symposium on Electrical Insulation, Boston, pp. 542-545 April 7-10, 2002.

[2] C.R. Paul, "Decoupling the multiconductor transmission line equations", IEEE Trans. on Microwave Theory and Techniques, Vol. 12, No. 1, pp. 1429-1440, August 1996.

[3] P.A.A.F. Wouters and P.C.J.M. van der Wielen, "Implications of on-line PD measurement on phase distributions for three-phase MV cables", 7th International Conference on Properties and Applications of Dielectric Materials, Nagoya, June 1-5, 2003.

[4] P.A.A.F. Wouters and P.C.J.M. van der Wielen, "Effect of cable load impedance on coupling schemes for MV power line communication", submitted to IEEE Bologna Power Tech 2003, Bologna, June 23-26, 2003.

[5] J.M. Wetzer and P.C.T. van der Laan, "Prebreakdown currents: basic interpretation and time-resolved measurements", IEEE Trans. on Electrical Insulation, Vol. 24, No. 2, pp. 297-308, April 1989.

**Author address:** Peter Wouters
Eindhoven University of Technology
Faculty of Electrical Engineering
Electrical Power Systems group, EVT-EPS
P.O.Box 513, 5600 MB Eindhoven
The Netherlands
E-mail: p.a.a.f.wouters@tue.nl
Tel: +31 40 2474244; fax: +31 40 2450735